

Learn2Reg: comprehensive multi-task medical image registration challenge, dataset and evaluation in the era of deep learning

Alessa Hering*, Lasse Hansen*[†], Tony C. W. Mok, Albert C. S. Chung, Hanna Siebert, Stephanie Häger, Annkristin Lange, Sven Kuckertz, Stefan Heldmann, Wei Shao, Sulaiman Vesal, Mirabela Rusu, Geoffrey Sonn, Théo Estienne, Maria Vakalopoulou, Luyi Han, Yunzhi Huang, Mikael Brudfors, Yaël Balbastre, Samuel Joutard, Marc Modat, Gal Lifshitz, Dan Raviv, Jinxin Lv, Qiang Li, Vincent Jaouen, Dimitris Visvikis, Constance Fourcade, Mathieu Rubeaux, Wentao Pan, Zhe Xu, Bailiang Jian, Francesca De Benetti, Marek Wodzinski, Niklas Gunnarsson, Jens Sjölund, Huaqi Qiu, Zeju Li, Christoph Großbröhmer, Andrew Hoopes, Ingerid Reinertsen, Yiming Xiao, Bennett Landman, Yuankai Huo, Keelin Murphy, Nikolas Lessmann, Bram van Ginneken, Adrian V. Dalca, Mattias P. Heinrich

Abstract—Image registration is a fundamental medical image analysis task, and a wide variety of approaches have been proposed. However, only a few studies have comprehensively compared medical image registration approaches on a wide range of clinically relevant tasks, in part because of the lack of availability of such diverse data. This limits the development of registration methods, the adoption of research advances into practice, and a fair benchmark across competing approaches. The Learn2Reg challenge addresses these limitations by providing a multi-task medical image registration benchmark for comprehensive characterisation of deformable registration algorithms. A continuous evaluation will be possible at <https://learn2reg.grand-challenge.org>. Learn2Reg covers a wide range of anatomies (brain, abdomen, and thorax), modalities (ultrasound, CT, MR), availability of annotations, as well as intra- and inter-patient registration evaluation. We established an easily accessible framework for training and validation of 3D registration methods, which enabled the compilation of results of over 65 individual method submissions from more than 20 unique teams. We used a complementary set of metrics, including robustness, accuracy, plausibility, and runtime, enabling unique insight into the current state-of-the-art of medical image registration. This paper describes datasets, tasks, evaluation methods and results of the challenge, and the results of further analysis of transferability to new datasets, the importance of label supervision, and resulting bias.

Index Terms—Medical Image registration, Evaluation, Grand Challenge

I. INTRODUCTION

Image registration is a fundamental task in medical image analysis and has been an active field of research for decades [1], [2], [3], [4]. Most studies that compared registration methods were focused on specific tasks or algorithmic aspects, and did not comprehensively characterise current approaches. With the recent success of deep learning

strategies in image analysis, the degree and dependency of algorithms on (partially) labelled training data is often a crucial aspect in current research. The Learn2Reg challenge aims to gain insight into which methodological components and supervision strategies are best suited for a wide range of clinically useful 3D image registration tasks, and sets a new benchmark to evaluate and distinguish strengths and weaknesses of task-tailored solutions. Learn2Reg covers a wide range of anatomies (brain, abdomen and thorax), modalities (ultrasound, CT, MRI, populations) and auxiliary annotations (e.g. segmentation, keypoints). The challenge also includes both intra- and inter-patient registration tasks. Due to this broad range, it serves as a unique benchmark to evaluate the current state-of-the-art with respect to various qualities of registration algorithms: accuracy, robustness, plausibility and speed. Furthermore, no other medical image registration challenge has thoroughly analysed the benefits and shortcomings of learning- and optimisation-based strategies. To engage a wider participation from new research groups, Learn2Reg removes entry barriers by providing pre-processed and pre-aligned images with additional annotations, as well as evaluation scripts and code for all evaluation metrics.

This overview ranks and scores results from over 65 entries from more than 20 teams throughout 2020 and 2021. We perform additional experiments to analyse the robustness towards cross-dataset transfer, the influence of the bias induced by only labelling certain anatomical regions, and direct comparisons of the supervision level of selected methods.

A. Related Work

In the following a brief overview of important related work on comparing (bio)-medical image registration, and its fundamental methodological choices that differentiate the wide range of metrics, optimisation, and supervision is given. General guidelines for setting up a fair and unbiased challenge have been recently thoroughly discussed in literature [5]. These criteria were adhered to in Learn2Reg and externally reviewed and confirmed by the MICCAI challenge team.

*Alessa Hering and Lasse Hansen contributed equally to this work.

[†]Corresponding author: hansen@imi.uni-luebeck.de, Institute of Medical Informatics, Universität zu Lübeck, Ratzeburger Allee 160, 23564 Lübeck, Germany

Author affiliations are listed at the end of the paper.

Challenges: There have previously been four prominent challenges for (bio)-medical image registration. Three challenges were single-task focused challenges: EMPIRE10 (lung CT), CuRIOUS (intra-operative US and MRI), and ANHIR (histology). Each attracted at least 10 participating teams and used various metrics for quantifying the performance. The EMPIRE10 challenge provided the most comprehensive evaluation including distances of manual landmark pairs, fissure segmentations, and Jacobian determinant values of the deformation field. This challenge also required (original) participants to perform live registrations during the MICCAI workshop in Beijing and therefore employed a time constraint on the computations. The Continuous Registration Challenge co-organised with WBIR 2018 aimed at combining multiple tasks from previous benchmarks (lung CT and inter-patient brain MRI). It addressed assessing registration quality as a service but is limited to algorithms that can be incorporated into the SimpleElastix framework and therefore had limited participation.

Benchmark Papers: Several papers have compared multiple registration algorithms for a given dataset. In contrast to challenges, these benchmark papers did not have (at least originally) an open workshop format that enabled wide-spread participation. Nevertheless, their findings provided meaningful insights. Starting from RIRE [6], which compared rigid-body alignment of head MRI (T1, T2), PET and CT, there have been several brain registration benchmarks - most notably the evaluation of 14 nonlinear iterative registration algorithms [7]. Fewer studies analyzed abdominal registration, and included the evaluation of six affine and non-linear algorithms on inter-patient registration of the "beyond the cranial vault" dataset [8]. This study revealed large performance gaps and motivated our inclusion of this dataset to study the potential benefit of supervised (learning-based) algorithms. The DIR-Lab datasets [9] have been widely used to benchmark intra-patient CT lung motion estimation and provide a leaderboard for state-of-the-art comparison. All landmarks are publicly available, which makes the dataset prone to overfitting on the test data.

Survey Papers and Baseline Methods: Surveys on conventional medical image registration [2], [3] have comprehensively reviewed typical categories of approaches including similarity metric, regulariser, and optimiser criteria. Due to the strong increase in the number of deep-learning-based registration paper in the last few years, several new surveys have been published (e.g. [4]) extending the typical categories with deep-learning specific categories like supervision-type and network architecture. Moreover, the training data and thus the registered body region and image modality are more important for deep-learning-based methods and get more into the focus of those survey papers. While few papers have evaluated their proposed registration method on more than two different registration tasks, there is a variety of public methods SyN [10], Elastix [11], NiftyReg [12] and deeds [13], and Voxelmorph [14] that are commonly used as baseline or comparison methods. When comparing only among deep-learning based methods simply re-training specific architectures on new data may be insufficient. Hence the use of

a challenge benchmark that incorporates several generally applicable baselines is essential for a fair evaluation.

B. Contributions

Learn2Reg provides both datasets and an easily accessible benchmark for the first comprehensive evaluation of a wide-range of methods for inter- and intra-patient, mono- and multimodal medical registration. We introduce a complementary set of metrics, including robustness, accuracy, plausibility and speed, that follows the principles defined by the BIAS group [5] and could become a de-facto benchmark for new algorithms. Further analysis of label bias (for supervised methods), domain transfer and statistical testing of significant differences across algorithms and types of methods highlight the complementary strength and weaknesses of learning vs. non-learning-based approaches.

II. MATERIAL AND METHODS

A. Challenge Organisation

The Learn2Reg challenge is organised by Alessa Hering (Fraunhofer MEVIS, Germany and Radboudumc Nijmegen, The Netherlands), Lasse Hansen (Institute of Medical Informatics, Universität zu Lübeck, Germany), Adrian Dalca (Computer Science and Artificial Intelligence Lab, MIT, USA) and Mattias Heinrich (Institute of Medical Informatics, Universität zu Lübeck, Germany) and is associated with the MICCAI 2020 and MICCAI 2021. The Learn2Reg challenge consists of two phases (mainly organised on grand-challenge.org).

- Phase 1 - Validation Phase: The participants downloaded the training and validation scan pairs for each task described in section II-B. The participants trained a registration network or tuned hyperparameters on the training scan pairs in their own facilities. The developed algorithms were used to register the scan pairs of the validation dataset. The resulting displacement fields on the validation dataset were submitted and evaluated using grand-challenge.org. Challenge participants were allowed to create five submissions per day to this phase.
- Phase 2 - Test phase: Within one week after the test data release, the participants had to send either the generated displacement fields to the organisers or a Docker container containing the algorithm. A Docker submission was preferred and made more attractive by evaluating the runtime of the algorithm.

To remove entry barriers for new participants with expertise in deep learning but not necessarily registration, the organisers provided pre-preprocessed data (resample, crop, pre-align, etc.). A detailed description of the used preprocessing is given in section II-B. Furthermore, the python evaluation code for voxel displacement fields as well as a example dockerfile were provided. Members of the organizers' institutes could participate in the challenge but were not eligible for awards. A continuous evaluation for validation and test data will be possible at grand-challenge.org¹.

¹<https://learn2reg.grand-challenge.org>
<https://learn2reg-test.grand-challenge.org>

B. Tasks

Learn2Reg consists of six clinically relevant complementary tasks (datasets). Table 1 summarises the dataset details, and we discuss them in detail below.

CuRIOUS: EASY-RESECT [15] is a simplified subset of the original RESECT dataset [16], previously used in the MICCAI CuRIOUS challenges [17]. The dataset contains 22 training and 10 testing subjects with low-grade brain gliomas, intended to help to develop MR vs. US registration algorithms to correct tissue shift in brain tumor resection. For the Learn2Reg challenge, we included T1w and T2-FLAIR MR scans, and spatially tracked intra-operative ultrasound volumes. All scans were acquired for routine clinical care of brain tumor resection procedures at St Olavs University Hospital (Trondheim, Norway). Matching anatomical landmarks were annotated between T2-FLAIR MR and 3D ultrasound volumes [16] to enable evaluation of the registration accuracy. During pre-processing, for each subject, the T1w scan is rigidly registered to the T2-FLAIR scan, and both scans are resampled to the same coordinate space as the 3D ultrasound volume yielding fixed voxel dimensions for all scans ($256 \times 256 \times 288$) at an isotropic resolution of approximately 0.5 mm.

Hippocampus MR: This dataset consists of 394 MR scans of the hippocampus region acquired in 90 healthy adults and 105 adults with a non-affective psychotic disorder taken from the Psychiatric Genotype/Phenotype Project data repository at Vanderbilt University Medical Center (VUMC). The hippocampus head and tail were manually traced in all scans. Previous to the Learn2Reg challenge, the dataset was used as part of the Medical Segmentation Decathlon [18].

Abdomen CT-CT: This task tackles inter-patient registration of abdominal CT scans, which enables statistical modelling of variations of abdominal organs for abnormality detection, and can provide a canonical atlas space for further investigations. The dataset contains 50 abdominal CT scans (30 for training, 20 for testing) with 13 manually labelled anatomical structures: spleen, right kidney, left kidney, gall bladder, esophagus, liver, stomach, aorta, inferior vena cava, portal and splenic vein, pancreas, left adrenal gland and right adrenal gland [8]. The images were registered affinely in a groupwise manner and resampled to the same voxel resolution and spatial dimensions ($192 \times 160 \times 256$).

Abdomen MR-CT: The dataset was compiled from public studies of the cancer imaging archive (TCIA) that contained paired scans of both MRI and CT from the same patients. In particular, 16 MRI and CT scans from the following studies, TCGA-KIRC, TCGA-KIRP, and TCGA-LIHC, are included in Learn2Reg - that cover routine diagnostic scans and follow-up imaging for kidney surgery (donation). The data has been reorientated, resampled to an isotropic resolution of 2 mm, and cropped and padded to achieve voxel dimensions of $192 \times 160 \times 192$. We have also manually traced 3D segmentation masks for the liver, spleen, left and right kidney. All scans were pre-aligned using a groupwise affine registration based on the deeds-linear algorithm. Additional unpaired and segmented training data from two further challenges: BCV-CT (see II-B) and CHAOS-MR were provided for pre-training.

OASIS: The task employed 416 3D whole-brain MR scans from the Open access series of imaging studies (OASIS) [19], a cross-sectional MRI data study with a wide range of participants from young, middle-aged, nondemented, and demented older adults. We performed standard brain MR pre-processing including skull-stripping, normalisation, pre-alignment, and resampling [20]. Semi-automatic labels with manual corrections of 35 cortical and subcortical brain structures were generated using FreeSurfer [21].

Lung CT: The aim of the lung CT task was the registration of expiration to inspiration CT scans of the lung. The data consists of 20 training [22] and 10 test scan pairs [23]. The scans were acquired at the Department of Radiology at the Radboud University Medical Center, Nijmegen, The Netherlands. All pairs were affinely pre-registered and resampled to an image size of $192 \times 192 \times 208$. Lung segmentation masks and keypoints were provided as additional training information.

C. Challenge Design

To provide a comprehensive evaluation of the registration performance, we consider a number of complementary metrics (see section II-C1) that assess the accuracy, robustness, plausibility, and speed of the algorithms. For final task ranks, we further consider the significance of differences in results. The detailed ranking scheme is described in section II-C2.

1) Metrics:

DSC: The Dice similarity coefficient (DSC) measures the overlap of two sets of segmentation labels (on the fixed and warped moving scan).

DSC30: To assess robustness, the DSC30 metric considers the 30th percentile in DSC scores over all cases. For the Abdomen CT-MR task, this robustness metric is replaced with a standard DSC on additional anatomical labels, that were not available during training (DSC9).

HD95: The Hausdorff distance (HD) indicates the maximum distance in a metric space (here: Euclidean space, distance specified in millimeters (mm)) between two sets of surfaces (segmentation labels on the fixed and warped moving scan). For a robust score, we consider the 95th percentile instead of the maximum distance (HD95).

TRE: The target registration error (TRE) is defined as the euclidean distance (in millimeters (mm)) between corresponding landmarks in the fixed and warped moving scan.

TRE30: Similar to the DSC30 score the TRE30 metric collects the 30th percentile of largest landmark distances.

SDlogJ: The plausibility (smoothness) of a displacement field is captured using the standard deviation of the logarithm of the Jacobian determinant (SDlogJ) of the displacement field ([24], [25]).

RT: In addition, we are able to measure the test-time registration runtime (RT) on the same hardware (CPU: Xeon Silver 4210R, GPU: Quadro RTX 8000), when methods are submitted as a docker container. Start and stop times are the loading of the first scan and writing of the displacement field to disk, respectively.

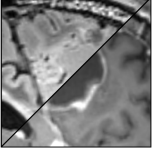
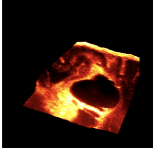












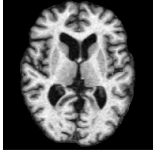
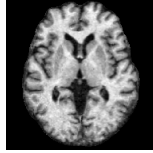
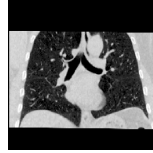
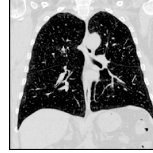









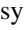
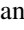
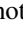
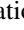
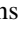
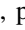
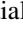
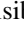
	CuRIOUS		Hippocampus MR		Abdomen CT-CT	
	Fixed	Moving	Fixed	Moving	Fixed	Moving
						
Modalities	MR T1w & FLAIR/US		MR T1w/MR T1w		CT/CT	
Intra-/Inter-patient	Intra-patient		Inter-patient		Inter-patient	
Resolution	256×256×288		64×64×64		192×160×256	
Voxel size	~0.5×0.5×0.5mm		1×1×1mm		2×2×2mm	
Cases (Train/Test)	32 (22/10)		394 (263/131)		50 (30/20)	
Preprocessing	resample		crop/pad/resample		canonical affine pre-align crop/pad/resample	
Annotations	9-18 landmarks/case		2 anatomical labels		13 anatomical labels	
Additional data						
Challenges	  				 	
	Abdomen MR-CT		OASIS		Lung CT	
	fixed	moving	fixed	moving	fixed	moving
						
Modalities	MR T1w / CT		MR T1w / MR T1w		CT / CT	
Intra-/Inter-patient	Intra-patient		Inter-patient		Intra-patient	
Resolution	192×160×192		160×192×224		192×192×208	
Voxel size	2×2×2mm		1×1×1mm		1.75×1.25×1.75mm	
Cases (Train/Test)	16 (8/8)		455 (416/39)		30 (20/10)	
Preprocessing	canonical affine pre-align crop/pad/resample				affine pre-align crop/pad/resample	
Annotations	4-9 anatomical labels		35 anatomical labels		100 landmarks/case	
Additional data	90 unpaired MR/CT scans ROI masks				lung masks	
Challenges	   				   	


TABLE I: Overview of all six Learn2Reg tasks addressing the imminent challenges of medical image registration: multi-modal scans , few/noisy annotations , partial visibility , small datasets , large deformations , small structures , unsupervised registration  and missing correspondences .

2) *Ranking Scheme*: We rank methods using statistically significantly different results. For each metric applied in a task, methods are compared against each other (Wilcoxon signed rank test with $p < 0.05$), ranked based on the number of "won" comparisons and finally mapped to a numerical metric rank score between 0.1 and 1 (with possible score sharing). A task rank score is then obtained as the geometric mean of individual metric rank scores. All methods for which no metric is available (not submitted to the task, no Docker container submitted) share the lowest possible metric rank score of 0.1.

III. CHALLENGE ENTRIES

In phase 1, performed using the grand-challenge.org platform, 17 teams submitted displacement fields in 2020 and 22

teams in 2021. In phase 2, two teams submitted displacement fields in 2020 and eight teams submitted their algorithms as docker images. In 2021, three teams submitted displacement fields and 12 teams submitted a docker. Only algorithms that participated in both phases of at least one year were included in this paper. Below is a brief description of each of the 21 algorithms. Table II provides a summary of important information for each algorithm. For a more detailed description of the algorithms, please refer to the respective articles, in the proceedings of the MICCAI Learn2Reg workshops [26].

3Idiots : [27] employ a hybrid similarity loss consisting of intensity (SSD), statistical (MI), and label-based (Dice + L1) penalties. A Voxelmorph model with an increased number of feature channels and halved output resolution is trained in a patch-wise manner and applied to the OASIS task.

	Tasks						Type	Objectives						Reg.	Optimis.	Misc. (used architectures, add. objectives, etc.)					
	CuRIOUS	Hippocampus MR	Abdomen CT-CT	Abdomen MR-CT	OASIS	Lung CT	Conventional	Deep Learning	NCC	MIND-SSC	NGF	MI	Dice	Keypoints	Consistency (Inv./Cycl.)	Diffusion	Curvature	Adam	Convex	L-BFGS/Gauss-Newton	
3Idiotis						●		●				●	●			●		●			Voxelmorph; SSD;
Bailiang						●		●	●				●			●		●			DeepRegNet;
ConvexAdam	■	●	●				○	○		○			○		○	●		○	○		UNet; Dense corr.;
corrField	■	■	■	■	■	■	●			●					●	●					Dense corr.;
Driver					●	●		●	●			●	○	○				●			PCNet; Cross-entropy loss;
Epicure						■	●		●												Bending energy regularisation;
Estienne		●	●					●	●				●			●		●			UNet; Multi-Task learning;
Gunnarsson	■	●	●			■		●	●				●			●		●			PWC;
Imperial				●	●	■		●			●		●	●		●		●			Structure-guided loss;
Joutard			●					●					●			●		●			UNet; EDT similarity; Dense corr.;
LapIRN	■	●	●	●	●	■	○	○	●	○		○	○			●		●			UNet; Conditional NN;
LaTIM				■	■	■	●														Directional representations;
Lifshitz						■		●	●						●						Unrolled L_1 regulariser; Dense corr.;
IWM		●			●			●		●			●		●	●		●			2-stream NN;
MEVIS	■	●	■	■	■	■	○	○			●		○	○			●	○		○	● Groupwise registration; Bayesian modelling;
Multi-brain				■	■	■	●									●					Bending and Jacobian regularisation;
NiftyReg	■	■	■	■	■	■	●		○	○											Dense Corr.;
PDD-Net	■	●	●			■		●		●			○			●		●			UNet; SSTVD similarity; Dense corr.;
PIMed			●	●	●	■	○	○	●				○					○			
Thorley					●		●									●					Voxelmorph;
Winter				■	■	■	○	○	●	●		●				●		●			

TABLE II: Methodological overview of all Learn2Reg methods. An entry in the table indicates agreement with the corresponding heading. Unsupervised and supervised challenge entries are marked with a ■ and ● symbol in the *Tasks* subgroup. If a challenge entry uses different approaches for different tasks or mixes them within the method (e.g. Deep Learning + Instance Optimisation) we marked the property with a ○ symbol. For detailed descriptions of the methods see Section III and the associated references.

Bailiang ■: [28] addressed OASIS and is based on the DeepRegNet framework from Project-MONAI. The input of the encoder is the concatenation of fixed and moving images. A dense vector field (DVF) is predicted from summing over different level decoders and integrated using scaling and squaring. The loss function is composed of LNCC, MIND-SSC, Dice, and a diffusion regulariser. https://github.com/BailiangJ/learn2reg2021_task3

ConvexAdam ■: [29] propose a decoupling of deep learning for semantic feature extraction, using an nnUNet, and a very fast and accurate conventional optimisation. They combine a single-level dense discretised displacement correlation with large capture range and convex global optimisation with a local gradient-based instance refinement using the Adam optimiser. The method is applied to all six tasks and uses diffusion regularisation, an inverse-consistency constraint, and MIND similarity, which is applicable for multi-modal and same-modality intra-patient alignment. The method extends the input features to learned label-supervised representations for inter-patient tasks: Abdomen CT-CT, Hippocampus, and OASIS brain. <https://github.com/multimodallearning/convexAdam>

corrField ■: A fast implementation (from [30]) of the corrField method [31] is introduced as a non-learning based unsupervised baseline. The method estimates sparse correspondences on image-based Förstner keypoints with exact message passing on a minimum spanning tree. MIND-SSC features are used for the similarity term. <https://grand-challenge.org/algorithms/corrfield/>

Driver ■: [32] use a dual-encoder U-net backbone with separated multi-scale feature extractors that comprises Deformation Field Integration (DFI) and non-rigid feature fusion (NFF) module. It produces multi-scale sub-fields that progressively align fixed and moving features. The DFI module integrates sub-fields through up-sampling, re-weighting, and warping operations. The NFF dynamically fuses features of three pathways based on attention mechanisms. The overall framework comprises a rigid transform network and MI or LNCC similarity, weak label-supervision and regularisation.

Epicure ■: [33] addresses the lung CT task using a conventional iterative-based registration approach based on Elastix toolbox optimizing the object function that is composed of the NCC similarity and a bending energy penalty term.

Estienne ■: [34], [35] addressed Abdomen CT-CT and Hippocampus with label-supervision. The method combines a diffeomorphic symmetric spatial transformer network with an embedding merging step, that eases the learning by subtracting the embeddings of separately encoded fixed and moving scans and thereby leveraging the prior knowledge that swapped inputs should yield negated velocity fields. They extend the label-based pre-training by including additional public datasets with at least partial overlap in segmentation classes, using segmentation masks produced by a CNN. https://github.com/TheoEst/abdominal_registration

Gunnarsson ■: [36] propose an end-to-end learning-based 3D registration method inspired by the PWC-Net [37]. The method estimates and refines a displacement field from a cost volume at each level of a CNN downsampling pyramid and is supervised by a similarity (NCC) and/or segmentation (DICE) loss, as well as a smoothness penalty. The network is trained and evaluated on scan pairs from three tasks of the 2020 challenge (Lung CT, Abdomen CT-CT and Hippocampus MR) using the same weights for all tasks. <https://github.com/ngunnar/learning-a-deformable-registration-pyramid>

Imperial ■: [Imperial] uses Image-and-Spatial Transformer Networks (ISTN) as the backbone of their method. In the ISTN, the fixed and moving images are first separately processed by the ITN to generate a segmentation mask and a feature map of the input image. Subsequently, both feature maps are used by the STN to predict the displacement field. The loss function consists of a structural-guided and image similarity and a regularisation loss. <https://github.com/biomediamira/istn>

Joutard ■: Joutard addresses the Abdomen CT-CT task with a weakly supervised deep learning approach. A CNN extracts features from the fixed and moving image, which are concatenated with their spatial image coordinates. The feature distributions for each spatial location are then matched between the two images which yield a correspondence matrix from which the average displacement can be derived. The network is supervised by a segmentation (Dice) and a regularisation (L2 norm on gradients) loss.

LapIRN ■: [38], [39] propose an image registration method based on Laplacian pyramid registration networks to overcome the large inter-and intra-variations of anatomical structures in the input scans. In 2021, [39] extended their approach by adding a conditional module that enables the input of the regularisation hyperparameter so that the different solutions for different hyperparameter values can be captured by a single convolutional neural network. This fast method won the on-site challenge in both years with robust results across all tasks. https://github.com/cwmok/Conditional_LapIRN

LaTIM ■: [40] is an iterative technique exploiting vector-valued directional image representations: smooth edge-based fields oriented towards the main image edges (closely related to vector field convolution for active contour segmentation). The method is implemented within the Elastix framework and shows improvements compared to directly using intensities.

Lifshitz ■: [41] propose a novel solution of learning-based lung CT registration that comprises a 3D extension of

ARFlow with multi-resolution warping, dense displacement correlation, and flow estimation. To address edge-preservation of sliding motion an unrolling of the total variation (L1) regularisation loss computation using variable substitution is proposed and shown to stabilise gradients during training.

IWM ■: The method of IWM submitted to the Hippocampus MR task uses sequential deformation field composition, while the solution for the OASIS task uses an image pyramid separately applied to both input images and a U-Net with residual blocks. The objective function includes MIND, Dice, inverse consistency and diffusion losses.

MEVIS ■: The submission of MEVIS [42] solves all tasks by classical iterative methods and build on cost functions and losses made up from several terms that are selected for the specific task. The methods use a coarse-to-fine multi-level iterative registration scheme where a Gaussian image pyramid is generated for both images to obtain downsampled and smoothed images. Then, a registration is performed on the lowest resolution level and the resulting deformation field serves as the starting point for the following registration on the next highest level. This proceeds to the finest level with quasi-Newton L-BFGS optimization at each level. For the Hippocampus task, a deep learning approach with a weakly supervised trained U-Net was applied using the same cost function as in the iterative approach.

Multi-brain ■: [43] use groupwise, fully unsupervised registration techniques based on Bayesian modelling and Gauss-Newton optimisation, which learns priors over image intensities and spatial tissue classes. The method requires no pre-processing of the imaging data and does not utilise label information. The method is applied to Abdomen CT-MR, OASIS, and Lung CT. <https://github.com/WTCN-computational-anatomy-group/mb>.

NiftyReg ■: [12] is applied as conventional baseline for all tasks without label supervision using NCC for CuRIOUS and otherwise MIND as similarity metric. Both bending and Jacobian regularisation penalties are applied and the number of pyramid levels is restricted to yield competitive run times (on multi-core CPU). <https://github.com/KCL-BMEIS/niftyreg>

PDD-Net ■: The PDD-Net (probabilistic dense displacement network) [44], [45] uses a compact deformable convolutional network to extract image features and compute a six-dimensional dissimilarity tensor (three spatial + three displacement dimensions). A smooth displacement field is obtained from the dissimilarities by interleaved (and twice repeated) steps of mean field inference over spatial dimensions and approximated min-convolutions over displacement dimensions. The method is adapted to four of the six challenge tasks (CuRIOUS, Hippocampus MR, Abdomen CT-CT, and Lung CT). https://github.com/multimodallearning/pdd_net

PIMed ■: PIMED use a multi-slice segmentation network and train a two-stage registration network for Abdomen CT-MR and Abdomen CT-CT and a residual VoxelMorph model for OASIS. For lung CT they apply a conventional method, with geodesic density regression and adaptation of intensities to lung tissue density [46].

Winter ■: Winter address all three tasks from 2021 by employing a traditional method for lung CT and a attention-

based DL registration for Abdomen CT-MR and OASIS brain. Improvements are found by a two-step approach that firstly aligns provided ROI masks. The algorithms achieve intermediate ranks for the considered tasks without using any label supervision. The smoothness complexity is large for abdominal registration. <https://github.com/WinterPan2017/ADLReg>

IV. ADDITIONAL EXPERIMENTS

Label Bias: Previous publications on learning-based registration have already discussed the possibility of introducing a bias towards anatomies that are used both for training and evaluation [47]. While this bias is intrinsic to all segmentation approaches, registration is often used as a more generalistic tool in clinical applications that may require accurate alignment of structures that are not defined a priori. To study the effect of adding additional anatomical labels to the evaluation that were not present during method development and training, we extended both abdomen tasks. For the inter-patient CT-CT registration we included the duodenum with the manual annotations provided by [48], for the intra-patient MR-CT task we extended the predominantly large organs by five smaller ones: gallbladder, stomach, aorta, portal vein, pancreas (semi-automatically generated using a specifically trained nnUNet).

Unsupervised Registration: The top-performing methods are all modular in their use of segmentation labels for supervision. As analysed in the label bias experiment, there is a risk of over-fitting registration performance to the chosen subset of manually annotated anatomies. We, hence, compared the unsupervised counterparts of the following methods: LapIRN and ConvexAdam. ConvexAdam already uses an unsupervised method for all three intra-patient tasks, and LapIRN for CuRIOUS and Lung CT. Therefore the additional comparisons are restricted to the abdomen and brain.

Transferability: A robust registration method should work well for all scan pairs regardless of acquisition parameters and thus on every comparable dataset. A frequently mentioned limitation of deep-learning-based methods is that they reach higher accuracy on the dataset they are trained on and show a considerable loss of accuracy on other data. As in [49], [50], we evaluate the transferability of the methods submitted to the lung CT-CT task by registering the DIRLab 4DCT [9] scan pairs. The DIRLab scans are preprocessed in the same way as the scans of the lung CT-CT task. The evaluation is based on the target registration error of the landmarks and the smoothness of the deformation field. Furthermore, this experiment allows comparison to a variety of other lung registration methods, as the DIRLAB data set is often used as a benchmark (please note that the reduced resolution leads to a general deterioration of TRE of around 0.2-0.3mm).

V. RESULTS

A. Challenge Outcome

In this section, we will first present and discuss each task separately and subsequently the eight methods that are included in the overall ranking being submitted to at least four of the six tasks. Tables III to VIII give the numerical results

and the scores for each algorithm for each task averaged over the number of scan pairs that were registered for that task. The algorithms are listed in order of their final placement per task. Fig. 1 shows boxplots illustrating the distribution of the accuracy (TRE and Dice) of the different methods for each task. Furthermore, for selected task (Abdomen MR-CT, OASIS, and Lung CT), a bubble chart combines the accuracy, smoothness, and runtime metric.

CuRIOUS: The registration to be carried out for this task was difficult for several reasons. First of all, it is a multimodal registration between MR and US images and the US images are typically noisier than the MR images. Furthermore, the pre-operative MR scans show a larger region of the brain whereas the intra-operative US volume was obtained to cover the entire tumor region after craniotomy but before dura opening. Due to these difficulties, only four methods were submitted to this task in addition to the three baseline methods. For two of these methods, some cases caused negative outliers and the average TRE was worse than the initial TRE (c.f. Table III). Only the two baseline methods corrField and PDD-Net as well as the ConvexAdam method registered all scan pairs satisfactorily.

Hippocampus MR: Due to its small volumetric size and reasonably large training dataset with only two anatomical labels, Hippocampus MR appeared to be a good entry-level task for learning-based registration approaches. It was also the only task that enabled sub-second run times. There was a performance gap between most supervised and unsupervised methods (NiftyReg, PDD-Net, and corrField). LapIRN reaches the first rank and MEVIS comes second, which notably used a fully-convolutional solution (without optimisation) only for this task. There is only a very small difference in the results between overall and robustness Dice (of the 30% most difficult instances), which highlights the fact that the problem is well-balanced and it requires fewer specific model adaptations.

Abdomen CT-CT: Considering the abdomen for inter-patient registration is more challenging than the brain, due to larger anatomical shape differences that require large, complex deformation estimation. Due to the small size of many organs and large initial misalignments, previous work has often reported accuracies of around 40% DSC or less for DL methods [51]. Here, learning-based approaches can leverage anatomical segmentation priors and reach substantial improvement over previous state-of-the-art (as reported in [8]). Estienne, LapIRN, and ConvexAdam achieved 67-69% Dice overlap (across 8 individual labels) nearly 20% points higher Dice scores than all other participants with less than 10 seconds runtimes each and reasonably smooth displacement fields ($SDLogJ < 0.2$). Unsupervised methods have the advantage of being independent of label bias and reach up to 49% overlap (corrField and PDD-Net).

Abdomen MR-CT: Multimodal nonlinear registration remains a challenging task in particular for abdominal scans where significant deformations can occur between scans as evident from low initial overlap of DSC-9=22% or DSC-4=33% (for 9 or 4 anatomical labels respectively). However, the provided initialisation masks can already lead to DSC-4>60% overlap using a similarity transform. The multimodal metrics, MIND [52] and NGF [53] were used by the majority

TABLE III: CuRIOUS

	TRE↓	TRE30↓	SDLogJ↓	RT↓	Rank↑
Initial	6.38	12.00			
corrField	2.84	5.29	0.00	2.70	0.85
PDD-Net	3.08	6.28	0.00	8.21	0.83
ConvexAdam	3.31	5.82	0.00	1.33	0.77
NiftyReg	4.09	7.85	0.00	23.1	0.56
LapIRN	5.67	11.1	0.00	34.8	0.49
MEVIS	6.55	10.4	0.00	57.8	0.42
Gunnarsson	7.1	10.1	0.14	42.2	0.19

TABLE V: Abdomen CT-CT

	DSC↑	DSC30↑	HD95↓	SDLogJ↓	RT↓	Rank↑
Initial	0.28	0.04	21.78			
ConvexAdam	0.69	0.45	11.03	0.06	2.75	0.94
LapIRN	0.67	0.47	12.51	0.12	3.80	0.82
Estienne	0.69	0.51	11.77	0.18	8.23	0.67
MEVIS	0.51	0.24	18.21	0.14	3.49	0.60
corrField	0.49	0.24	17.22	0.28	5.40	0.53
PIMed	0.49	0.23	15.75	0.05		0.49
PDD-Net	0.49	0.24	17.75	0.41	6.06	0.44
Joutard	0.40	0.13	17.25	0.05	3.67	0.42
NiftyReg	0.45	0.20	20.70	0.36	17.1	0.36
Gunnarsson	0.43	0.17	18.55	0.13	31.5	0.33

TABLE VII: OASIS

	DSC↑	DSC30↑	HD95↓	SDLogJ↓	RT↓	Rank↑
Initial	0.56	0.27	3.86			
LapIRN	0.82	0.66	1.67	0.07	1.21	0.92
ConvexAdam	0.81	0.64	1.63	0.07	3.10	0.82
IWM	0.79	0.61	1.84	0.05	2.55	0.79
Driver	0.80	0.62	1.77	0.08	2.02	0.75
PIMed	0.78	0.58	1.86	0.06	3.47	0.71
3Idiots	0.80	0.63	1.82	0.08	1.46	0.70
Winter	0.77	0.57	2.16	0.08	2.56	0.55
MEVIS	0.77	0.57	2.09	0.07	10.4	0.51
Multi-brain	0.78	0.59	1.92	0.57		0.38
corrField	0.74	0.51	2.36	0.08	5.14	0.37
Thorley	0.77	0.60	2.21	0.31		0.37
NiftyReg	0.73	0.51	2.37	0.06	5.00	0.36
Bailiang	0.67	0.42	2.74	0.04	1.38	0.33
LaTIM	0.74	0.52	2.31	0.08		0.32
Imperial	0.76	0.57	2.43	0.19	2610	0.29

TABLE IV: Hippocampus MR

	DSC↑	DSC30↑	HD95↓	SDLogJ↓	RT↓	Rank↑
Initial	0.55	0.36	3.91			
LapIRN	0.88	0.86	1.30	0.05	1.03	0.93
MEVIS	0.85	0.84	1.55	0.05	0.59	0.78
ConvexAdam	0.84	0.83	1.85	0.07	0.48	0.75
IWM	0.79	0.76	2.20	0.08	0.80	0.63
Estienne	0.85	0.84	1.51	0.09	1.46	0.62
PDD-Net	0.78	0.76	2.23	0.07	0.35	0.58
NiftyReg	0.76	0.72	2.72	0.09	4.75	0.37
corrField	0.72	0.68	2.89	0.05	1.20	0.34
Gunnarsson	0.74	0.67	2.82	0.16	22.0	0.25

TABLE VI: Abdomen MR-CT

	DSC↑	DSC9↑	HD95↓	SDLogJ↓	RT↓	Rank↑
Initial	0.33	0.22	48.65			
ConvexAdam	0.75	0.73	24.92	0.09	1.30	0.82
corrField	0.76	0.73	23.35	0.10	2.13	0.81
LapIRN	0.76	0.69	22.81	0.12	1.50	0.77
PIMed	0.78	0.68	21.99	0.07	59.2	0.75
MEVIS	0.71	0.65	27.94	0.15	14.7	0.67
Driver	0.76	0.55	27.02	0.13	1.95	0.63
NiftyReg	0.65	0.55	33.09	0.12	11.0	0.55
LaTIM	0.54	0.49	41.17	0.13		0.39
Winter	0.55	0.41	35.51	0.85	2.79	0.31
Imperial	0.51	0.41	48.60	0.11	278	0.30
Multi-brain	0.54	0.44	38.21	0.48		0.30

TABLE VIII: Lung CT

	TRE↓	TRE30↓	SDLogJ↓	RT↓	Rank↑
Initial	10.24	16.80			
corrField	1.75	2.48	0.05	2.91	0.87
ConvexAdam	1.79	2.70	0.06	1.82	0.81
MEVIS	1.68	2.37	0.08	95.4	0.78
LapIRN	1.98	2.95	0.06	10.3	0.73
PDD-Net	2.46	3.81	0.04	4.22	0.62
LaTIM	1.83	2.50	0.05		0.62
Lifshitz	2.26	3.01	0.07	2.90	0.61
Imperial	1.81	2.54	0.11	300	0.57
PIMed	2.34	3.27	0.04	623	0.55
NiftyReg	2.70	5.28	0.10	42.2	0.51
Driver	2.66	3.50	0.10	2.66	0.44
Winter	7.41	10.11	0.09	12.0	0.40
Epicure	6.55	10.29	0.07		0.29
Multi-brain	6.61	8.75	0.08		0.27
Gunnarsson	9.00	11.27	0.12	30.9	0.21

TABLE IX: Overall rank scores of methods submitted to four or more tasks.

	CuRIOUS	Hippocampus MR	Abdomen CT-CT	Abdomen MR-CT	OASIS	Lung CT	Overall	Intra-Patient	Inter-Patient
ConvexAdam	0.77	0.75	0.94	0.82	0.82	0.81	0.82	0.80	0.83
LapIRN	0.49	0.93	0.82	0.77	0.92	0.73	0.76	0.65	0.89
MEVIS	0.42	0.78	0.60	0.67	0.51	0.78	0.61	0.61	0.62
corrField	0.85	0.34	0.53	0.81	0.37	0.87	0.59	0.84	0.41
NiftyReg	0.56	0.37	0.36	0.55	0.36	0.51	0.44	0.54	0.36
PIMed			0.49	0.75	0.71	0.55	0.35	0.39	0.33
PDD-Net	0.83	0.58	0.44			0.62	0.34	0.37	0.32
Gunnarsson	0.19	0.25	0.33			0.21	0.19	0.16	0.22

of participants, including the two top-performing methods ConvexAdam and corrField. Those methods also capture larger motion robustly using dense discrete correlation. LapIRN and PIMed (3rd and 4th rank) added a Dice loss, where it became obvious that focusing on the supervision with only 4 organs may lead to over-fitting on those structures and a lower accuracy for further anatomies. The provided additional labeled unpaired datasets (30 BCV CT scans and 30 CHAOS MRI scans [54]) have not yielded the desired advantages due to subtle differences in appearance.

OASIS: The OASIS inter-subject brain task attracted the most learning-based solutions. The results are summarised in Table VII and visualised in Fig. 1 showing that most of these methods achieve very similar results in terms of Dice Score for the cases with the highest scores (Dice of 80-90%). The differences are primarily in the more difficult cases and thus in the DSC30 score, where the LapIRN, convexAdam, and the methods of Driver and 3idiots methods perform slightly better than for example PIMed and Winter. The conventional methods of MEVIS and corrField achieve mid-ranked accuracies but have a higher runtime. Fig. 2 shows an example sagittal slice of the fixed image overlayed with the false-negative segmented voxels (green) and false-positive segmented voxels (yellow) for initial moving segmentation and the propagated segmentations by the methods of Imperial, PIMed, and LapIR. All methods were able to align the small structures of the brain with only very small visible differences.

Lung CT: The complexity of this registration task is manifold. First, the fields of view of the fixed and moving scan differ largely since the lungs in the expiration scan are not fully visible. Second, the scale of the motion within the lungs can often be larger than the anatomical structures (vessels and airways) themselves. Therefore, a registration method needs to estimate large displacements that account for substantial breathing motion and also align small structures like individual pulmonary blood vessels precisely. To measure the accuracy manual landmarks are used that are typically located at the boundary or bifurcation of vessels, airways, and parenchyma. This task was carried out in both years because in 2020 only the MEVIS team, which uses automatically computed keypoints as additional metric, achieved a TRE of less than 2mm (1.72mm), while other teams performed considerably worse (e.g. LapIRN 3.24mm and PDD-Net 2.46mm). In 2021, keypoint correspondences were provided for training and the submissions improved with six teams achieving a TRE of less than 2mm. Especially for the deep-learning-based methods LapIRN and Imperial this is a remarkable result, because they were only trained on a small dataset of 20 scan pairs. In contrast to other lung registration challenges like EMPIRE or DIRLab, the TRE is relatively high. This can be explained, in part, by the low resolution of the scans that were chosen in the preprocessing. Fig. 2 visualises the difference images of an example coronal slices for the methods of Driver, convexAdam, and MEVIS overlayed with the landmarks.

Overall Ranking: ConvexAdam was among the top 3 on each task (winning Abdomen CT-CT and Abdomen CT-MR) and ranked first overall among the eight methods that were applied to four or more tasks - highlighting the importance of

effective optimisation and versatility of using learned semantic or hand-crafted MIND features depending on the application. LapIRN reached the overall second rank and yielded the best result for Hippocampus and OASIS. This demonstrates that a well-designed convolutional feed-forward network (instance optimisation was used only for CuRIOUS and Lung CT) can outperform conventional approaches in particular for inter-patient tasks. MEVIS achieved the third place overall, with top ranks in particular for Lung CT and Hippocampus based on a combination of NGF metric, curvature regularisation, and L-BFGS optimisation with additional learning components only employed for the brain task. CorrField uses no label supervision at all, but relies on highly optimised graph-based registration, and comes fourth overall winning two individual tasks: CuRIOUS and LungCT. It is the best method for intra-patient registration. PIMed's method achieves strong performance on Abdomen MR-CT and OASIS and generalises well to Abdomen CT-CT.

B. Additional Experiments

Label Bias and Unsupervised Registration: When evaluating the influence of supervision with anatomical labels, we found a clear distinction between intra-patient registration (Abdomen MR-CT) and inter-patient registration (Abdomen CT-CT, Hippocampus and OASIS). The former shows nearly no advantage of including such information and it is therefore possible to avoid a risk of overfitting towards certain anatomies. The latter, however, shows a clear deterioration in accuracy when excluding all or some of the structures from training that were used for evaluation. CorrField, which is unsupervised and achieves the highest scores for intra-patient registration trails nearly all learning-based methods on the remaining inter-patient tasks. LapIRN trained without Dice loss (i.e. without anatomical knowledge) improves upon those results and achieves very strong results for OASIS and Abdomen CT-CT (ranks would be third and fourth respectively). This demonstrates that in particular a large training database and an advanced deep learning architecture (LapIRN uses multi-level Res-Nets, multiple warps and multi-resolution loss functions) can narrow the gap between supervised and unsupervised approaches. We evaluated ConvexAdam (that decouples feature extraction from optimisation) for Abdomen CT-CT in three settings: 1) all 13 labels in training with 8 (7 identical) in test (DSC=69%), 2) 4 labels in training with 8 (thereof 3 identical) in test (DSC=55%) and 3) no labels in training (DSC=45%). This shows that partial supervision clearly leads to improvement of those identical anatomies but can also help to align nearby structures: esophagus which was excluded improved by 16% points (likely through the guidance of liver and aorta) and pancreas overlap was increased by 12% points (possibly by including portal vein and adrenal gland). As mentioned in Sec. V-A training on 4 and evaluating on 9 abdominal organs for MR-CT fusion results in a moderate performance gap between supervised and unsupervised methods (the latter being about 10% better on this metric).

Transferability: In this experiment, we were able to show that the three best methods of the lung registration

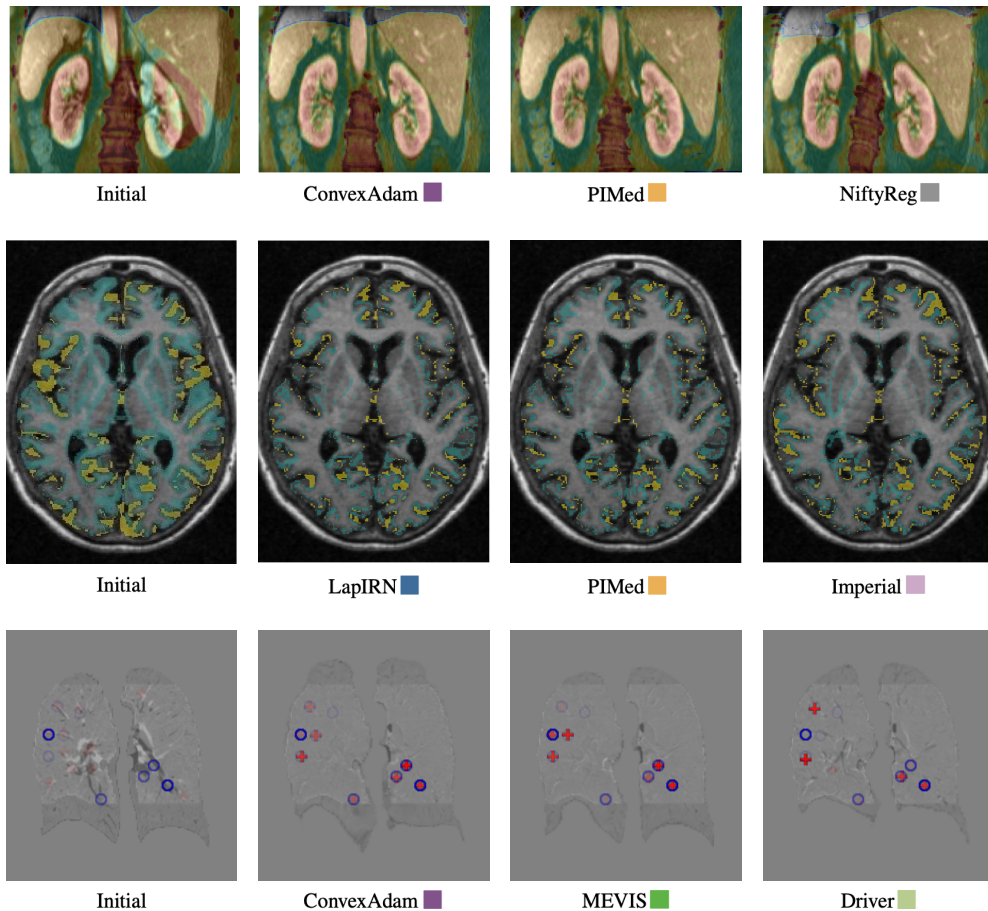


Fig. 2: Exemplary qualitative results for selected methods and tasks. Top row: Overlay of coronal abdominal MR (gray) and warped CT (color) slices. Middle row: False-negative (green) and false-positive (yellow) voxels of propagated segmentation labels on sagittal slices of the OASIS dataset. Bottom row: Coronal slices of difference images between exhale and warped inhale lung CT scans (including exhale (blue circle) and warped inhale (red cross) landmarks).

task also perform very well on the DIRLab dataset (MEVIS 1.22 mm, convexAdam 1.31 mm, and corrField 1.34 mm) without any further hyperparameter adaptations. Since the inspiration and expiration images of the DIRLab dataset are extracted from a 4DCT dataset with shallow breathing, the registration task is easier than the Learn2Reg lung CT task. Therefore, the methods reach a lower TRE on the DIRLab dataset compared to the Learn2Reg lung task (improved TRE of 0.46 mm, 0.48 mm, and 0.41 mm for MEVIS, convexAdam, and corrField, respectively). Due to the performed preprocessing and the reduced resolutions, the Learn2Reg methods achieve slightly worse results than state-of-the-art methods evaluated on the DIRLab dataset. For example, method of MEVIS included in a registration pipeline registering the original images reaches a TRE of 0.94 mm [55]. LapIRN achieves similar results on both datasets (Learn2Reg lung CT 1.98 mm and DIRLab 1.98 mm) showing that the best deep-learning-based methods can also be successfully applied to other datasets without retraining. However, no performance improvement can be observed on the easier dataset mainly due to the limited training data size.

VI. DISCUSSION

In the following, we will discuss specific aspects of the challenge.

Comparison of Learning- vs Optimisation-based Registration: We argue that Learn2Reg has helped to demystify common beliefs of fundamental differences between learning- and optimisation registration. First and foremost, there is virtually no difference in computational speed. GPU-acceleration brings down computation cost of optimisation-based methods to a few seconds for 3D registration, i.e. the extraction of features using CNNs often outweighs optimisation times. Furthermore, we see a clear trend that learning based on segmentation labels is primarily beneficial for inter-subject registration. For Abdomen CT-CT for instance large improvements of 20% points in Dice overlap compared to previous work [8] could be achieved when incorporating Dice losses. All three highest ranked approaches employ a combination of DL and optimisation: LapIRN primarily uses a deep network, but add instance optimisation for Lung CT, MEVIS mainly use conventional optimisation but a DL network for Hippocampus MR, and ConvexAdam combine discrete optimisation with UNet-based semantic features for inter-patient tasks. Our

current challenge design did not consider any computational constraints (GPU memory, inference time on CPU), which might limit the practical impact for some applications and should be considered in future studies.

Algorithmic Design Choices: There are no direct ablation studies possible for the used architectures and loss functions since each method differs in multiple aspects (see Table II), but some general trends are visible nonetheless. Most approaches use a combination of contrast-invariant intensity metrics (LNCC, NGF and MIND) as well as a Dice loss for tasks where anatomical labels are available. To address larger motion (all tasks expect brain) DL registration methods employ multi-scale (and residual) architectures, multiple warps or often dense correlation layers. Two-stream approaches that process both input scans independently are commonplace to deal with multimodality or contrast variations (lung CT).

Plausibility of Transformations: We analysed the smoothness of transformations with respect to the log-standard deviation of Jacobian determinants for all experiments. While this measure is far from perfect, it enabled a ranking of different solutions to the inherently ambiguous nonlinear registration task that may achieve similar accuracy with large differences in complexity (the common assumption being: the smoother transform is then preferable). As visualised in the bubble-charts in Fig. 1 there is a tendency that more accurate solutions are also smoother, which indicates that enforcing regularity is an effective means of avoiding overfitting and improves robustness. Some notable exceptions can be found for lung CT, where Imperial appears to suffer from too low regularisation while PDD-Net and PIMed may have reduced accuracy in exchange for overly smooth fields. A potential explanation for the positive correlation of smoothness and accuracy could be the hypothesis that accurate methods are able to establish strong (correct) correspondences at relevant anatomies and extrapolate as smooth as possible in uncertain areas. That means putting emphasis on either surfaces (e.g. based on segmentation estimates) or geometric keypoints (for lung scans) can be beneficial.

Comparison to Baselines: We evaluated two conventional methods, NiftyReg [12] and corrField [31] (using the GPU implementation of [30]), and two learning-based approaches, PDD-Net [44] and the original version of VoxelMorph [47] as baselines. The latter two were only applied to a subset of tasks. NiftyReg achieves reasonable accuracies across all tasks but falls behind supervised methods on inter-patient tasks. The original VoxelMorph variant reaches an average Dice overlap of $76.88\% \pm 2.17\%$ for OASIS (7th-10th place based on DSC alone) and a TRE of 7.51 ± 3.43 mm for lung CT (13th place). When trained on a large additional lung dataset [49] a TRE of 1.71 ± 2.86 mm was achieved for the additional DRLAB lung experiment for which the best performing methods in this challenge achieved 1.3 mm. PDD-Net achieved a second rank for CuRIOUS and fifth place for Lung CT, but lower scores for inter-patient registration. CorrField achieved the best scores overall for CuRIOUS and LungCT and second place for Abdomen MR-CT (each task without supervision), making it stand out as the best performing intra-patient approach. This demonstrates that conventional

methods are still very competitive for datasets without strong label supervision.

Reducing Entry Barriers: By pre-processing each dataset to the same dimensions and isotropic resolution and providing anatomical annotations for training data wide participation was achieved from research groups across the world. The OASIS inter-subject brain task attracted the most learning-based solutions, which highlights the importance of large, labeled training datasets for deep-learning-based registration and mirrors the focus of recent research. Lung CT intra-patient registration was addressed by the same number but more diverse set of methods, including conventional, fully deep-learning-based, and hybrid approaches. Therefore, we assert that new application areas have been opened for many participants. While adoptions of metrics, fine-tuning, and supervision appeared to be important for methods that were applied across multiple tasks, the consistent performance of the three top-performing groups demonstrates that Learn2Reg enabled effective multi-task solutions. Some aspects of medical image registration, including affine or rigid pre-alignment, dealing with differences in field-of-view of voxel resolutions, and the processing of very high-resolution scans have been omitted due to our challenge design and could be addressed in future.

Limitations of the Challenge Design: We have identified a number of limitations that should be addressed in future studies. First, for computational reasons the training of algorithms was performed offline by participants. This could introduce a bias when additional data is used by certain teams that is not accessible to others and prevents the use of larger (central) datasets that cannot be made public due to privacy concerns. Enabling docker-based training or fine-tuning of models directly at grand-challenge.org would be desirable. Second, the amount of available annotated training data varied across tasks and made in particular intra-patient tasks harder for learning-based approaches. Decoupling anatomical feature learning from patient-wise optimisation could be a next step, e.g. by providing training data for airway and fissure segmentation for lung CT. Third, the accuracy evaluation is in general limited by inter-observer noise and the difficulty of assessing registration accuracy based on segmentation overlap, which disregards the plausibility of correspondences along the surface or within the structure. Since this problem is inherent to any registration evaluation, we cannot offer any better solution than aiming for further manual annotation efforts. Fourth, the provision of all segmentation classes for training that were used for testing is in our opinion the most problematic limitation of this challenge. This was due to the fact, that for 3 out of 4 tasks with segmentation labels these annotations were already publicly available prior to Learn2Reg and we considered it in-transparent (and biased) to simply not point participants to their availability. While this would not be considered a problem at all for segmentation tasks (cf. the Medical Decathlon), image registration generally aims to recover deformations for the entire field-of-view. We aimed to mitigate the influence of over-fitting towards labelled anatomies by performing additional experiments for partial supervision.

Impact and Clinical Adoption: With regard to the five-year-old survey on medical image registration by [3], we can reflect that the shift from surface-based registration to intensity-based approaches has somewhat been reverted with a majority of approaches employing segmentation-based overlap or keypoints as driving force. The establishing of different learning-based strategies, including hybrid approaches that decouple semantic feature extraction from optimisation or combine feed-forward networks with instance optimisation, can be seen as an important new trend. To assess the likelihood of adopting registration in clinical practice, we are encouraged to see that a number of previous obstacles have been successfully addressed by participants of Learn2Reg. First, robustness against variations in scanner protocol and patient characteristics was shown to be very high for top-ranking methods that tackled both multi-centric MRI studies (OASIS) as well as the transferability issue for lung CT. Second, run times have been considerably reduced to a few seconds, which will enable clinicians to interact with those algorithmic solutions by adjusting hyper-parameters, e.g. the strength of regularisation penalties in near realtime (this holds only true for deep-learning-based methods if they are either decoupled or trained with conditioning cf. [39]). Third, it became clear that highly nonrigid transformations are as well solved as rigid alignment, opening up the promise for clinical applications in image-guided surgery, radiotherapy. In fact, it appears as if rigid/pre-alignment remains an active problem in particular for DL solutions.

VII. CONCLUSION

The Learn2Reg challenge was the first to evaluate a wide-range of methods for various inter- and intra-patient as well as mono- and multimodal medical image registration tasks. The main goal of this challenge was to provide a standardised benchmark on complementary tasks with clinical impact and a platform for comparison of conventional and learning-based medical image registration methods. We established a lower entry barrier for training and validation of 3D registration, which helped us compile results of over 65 individual method submissions from more than 20 unique teams. Although registration is highly dependent on the task, three methods (convexAdam, LapIRN, MEVIS) and a baseline method (corrField) were shown to work robustly on all tasks with only minor adjustments to the hyperparameters. Furthermore, several teams (Estienne, PIMed, Driver, 3idiots, Multi-brain LaTIM, Lifshitz and Imperial) have submitted tailored solutions to individual tasks and achieve very good results with it. For the conventional methods convexAdam, MEVIS, and corrField, it was also shown that they can be applied directly to new data sets without loss of accuracy. Furthermore, we demystified the common belief that conventional registration methods have to be much slower than deep-learning-based methods. Nevertheless, with LapIRN a deep-learning-based registration method achieves state-of-the-art registration results within seconds. We could not identify any architecture that was advantageous over others. However, it was found that for deep-learning-based methods using a Dice loss for inter-patient

registration is particularly useful and instance optimisation helped increasing the accuracy for intra-patient registration. With the Learn2Reg challenge, we have created a dataset for benchmarking future registration papers. Furthermore, the dataset has the potential to allow the development of dataset-independent and self-configuring registration methods.

REFERENCES

- [1] J. A. Maintz and M. A. Viergever, "A survey of medical image registration," *Medical image analysis*, vol. 2, no. 1, pp. 1–36, 1998.
- [2] A. Sotiras, C. Davatzikos, and N. Paragios, "Deformable medical image registration: A survey," *Medical Imaging, IEEE Transactions on*, vol. 32, no. 7, pp. 1153–1190, July 2013.
- [3] M. Viergever, J. Maintz, S. Klein, K. Murphy, M. Staring, and J. Pluim, "A survey of medical image registration—under review," *Medical Image Analysis*, vol. 33, pp. 140–144, 2016.
- [4] G. Haskins, U. Kruger, and P. Yan, "Deep learning in medical image registration: a survey," *Machine Vision and Applications*, vol. 31, no. 1, p. 8, 2020.
- [5] L. Maier-Hein, A. Reinke, M. Kozubek, A. L. Martel, T. Arbel, M. Eisenmann, A. Hanbury, P. Jannin, H. Müller, S. Onogur *et al.*, "Bias: Transparent reporting of biomedical image analysis challenges," *Medical image analysis*, vol. 66, p. 101796, 2020.
- [6] J. West, J. M. Fitzpatrick, M. Y. Wang, B. M. Dawant, C. R. Maurer Jr, R. M. Kessler, R. J. Maciunas, C. Barillot, D. Lemoine, A. Collignon *et al.*, "Comparison and evaluation of retrospective intermodality brain image registration techniques," *Journal of computer assisted tomography*, vol. 21, no. 4, pp. 554–568, 1997.
- [7] A. Klein, J. Andersson, B. A. Ardekani, J. Ashburner, B. Avants, M.-C. Chiang, G. E. Christensen, D. L. Collins, J. Gee, P. Hellier *et al.*, "Evaluation of 14 nonlinear deformation algorithms applied to human brain mri registration," *Neuroimage*, vol. 46, no. 3, pp. 786–802, 2009.
- [8] Z. Xu, C. P. Lee, M. P. Heinrich, M. Modat, D. Rueckert, S. Ourselin, R. G. Abramson, and B. A. Landman, "Evaluation of six registration methods for the human abdomen on clinically acquired ct," *IEEE Transactions on Biomedical Engineering*, vol. 63, no. 8, pp. 1563–1572, 2016.
- [9] R. Castillo, E. Castillo, R. Guerra, V. E. Johnson, T. McPhail, A. K. Garg, and T. Guerrero, "A framework for evaluation of deformable image registration spatial accuracy using large landmark point sets," *Physics in Medicine & Biology*, vol. 54, no. 7, p. 1849, 2009.
- [10] B. B. Avants, C. L. Epstein, M. Grossman, and J. C. Gee, *Medical image analysis*, vol. 12, no. 1, pp. 26–41, 2008.
- [11] S. Klein, M. Staring, K. Murphy, M. A. Viergever, and J. P. Pluim, "Elastix: a toolbox for intensity-based medical image registration," *IEEE transactions on medical imaging*, vol. 29, no. 1, pp. 196–205, 2009.
- [12] M. Modat, G. R. Ridgway, Z. A. Taylor, M. Lehmann, J. Barnes, D. J. Hawkes, N. C. Fox, and S. Ourselin, "Fast free-form deformation using graphics processing units," *Computer methods and programs in biomedicine*, vol. 98, no. 3, pp. 278–284, 2010.
- [13] M. P. Heinrich, M. Jenkinson, M. Brady, and J. A. Schnabel, "Mrf-based deformable registration and ventilation estimation of lung ct," *IEEE transactions on medical imaging*, vol. 32, no. 7, pp. 1239–1248, 2013.
- [14] A. V. Dalca, G. Balakrishnan, J. Guttag, and M. R. Sabuncu, "Unsupervised learning of probabilistic diffeomorphic registration for images and surfaces," *Medical image analysis*, vol. 57, pp. 226–236, 2019.
- [15] Y. Xiao, M. Fortin, G. Unsgård, H. Rivaz, and I. Reinertsen, "Easy-resect," 2020. [Online]. Available: <https://archive.sigma2.no/pages/public/datasetDetail.jsf?id=10.11582/2020.00025>
- [16] Y. Xiao, M. Fortin, G. Unsgård, H. Rivaz, and I. Reinertsen, "Retrospective evaluation of cerebral tumors (resect): A clinical database of pre-operative mri and intra-operative ultrasound in low-grade glioma surgeries," *Medical physics*, vol. 44, no. 7, pp. 3875–3882, 2017.
- [17] Y. Xiao, H. Rivaz, M. Chabanas, M. Fortin, I. Machado, Y. Ou, M. P. Heinrich, J. A. Schnabel, X. Zhong, A. Maier *et al.*, "Evaluation of mri to ultrasound registration methods for brain shift correction: the curious2018 challenge," *IEEE Transactions on Medical Imaging*, vol. 39, no. 3, pp. 777–786, 2019.
- [18] M. Antonelli, A. Reinke, S. Bakas, K. Farahani, B. A. Landman, G. Litjens, B. Menze, O. Ronneberger, R. M. Summers, B. van Ginneken *et al.*, "The medical segmentation decathlon," *arXiv preprint arXiv:2106.05735*, 2021.

- [19] D. S. Marcus, T. H. Wang, J. Parker, J. G. Csernansky, J. C. Morris, and R. L. Buckner, "Open access series of imaging studies (oasis): cross-sectional mri data in young, middle aged, nondemented, and demented older adults," *Journal of cognitive neuroscience*, vol. 19, no. 9, pp. 1498–1507, 2007.
- [20] A. Hoopes, M. Hoffmann, B. Fischl, J. Guttag, and A. V. Dalca, "Hypermorph: Amortized hyperparameter learning for image registration," in *International Conference on Information Processing in Medical Imaging*. Springer, 2021, pp. 3–17.
- [21] B. Fischl, "Freesurfer," *Neuroimage*, vol. 62, no. 2, pp. 774–781, 2012.
- [22] A. Hering, K. Murphy, and B. van Ginneken, "Learn2Reg Challenge: CT Lung Registration - Training Data," May 2020. [Online]. Available: <https://doi.org/10.5281/zenodo.3835682>
- [23] —, "Learn2Reg Challenge: CT Lung Registration - Test Data," Sep. 2020. [Online]. Available: <https://doi.org/10.5281/zenodo.4048761>
- [24] A. D. Leow, I. Yanovsky, M.-C. Chiang, A. D. Lee, A. D. Klunder, A. Lu, J. T. Becker, S. W. Davis, A. W. Toga, and P. M. Thompson, "Statistical properties of jacobian maps and the realization of unbiased large-deformation nonlinear image registration," *IEEE transactions on medical imaging*, vol. 26, no. 6, pp. 822–832, 2007.
- [25] S. Kabus, T. Klinder, K. Murphy, B. van Ginneken, C. Lorenz, and J. P. Pluim, "Evaluation of 4d-ct lung registration," in *International Conference on Medical Image Computing and Computer-Assisted Intervention*. Springer, 2009, pp. 747–754.
- [26] N. Shusharina, M. P. Heinrich, and R. Huang, Eds., *Segmentation, Classification, and Registration of Multi-modality Medical Imaging Data*. Springer International Publishing, 2021. [Online]. Available: <https://doi.org/10.1007/978-3-030-71827-5>
- [27] L. Han, H. Dou, Y. Huang, and P.-T. Yap, "Deformable registration of brain mr images via a hybrid loss," *arXiv preprint arXiv:2110.15027*, 2021.
- [28] DeepRegNet, "Deepregnet," 2021. [Online]. Available: <https://github.com/Project-MONAI/MONAI/blob/dev/monai/networks/nets/regunet.py>
- [29] H. Siebert, L. Hansen, and M. P. Heinrich, "Fast 3d registration with accurate optimisation and little learning for learn2reg 2021," 2021.
- [30] L. Hansen and M. P. Heinrich, "Graphregnet: deep graph regularisation networks on sparse keypoints for dense registration of 3d lung cts," *IEEE Transactions on Medical Imaging*, vol. 40, no. 9, pp. 2246–2257, 2021.
- [31] M. P. Heinrich, H. Handels, and I. J. Simpson, "Estimating large lung motion in copd patients by symmetric regularised correspondence fields," in *International conference on medical image computing and computer-assisted intervention*. Springer, 2015, pp. 338–345.
- [32] J. Lv, Z. Wang, H. Shi, H. Zhang, S. Wang, Y. Wang, and Q. Li, "Joint progressive and coarse-to-fine registration of brain mri via deformation field integration and non-rigid feature fusion," *arXiv preprint arXiv:2109.12384*, 2021.
- [33] C. Fourcade, M. Rubeaux, and D. Mateus, "Using elastix to register inhale/exhale intrasubject thorax ct: A unsupervised baseline to the task 2 of the learn2reg challenge," in *International Conference on Medical Image Computing and Computer-Assisted Intervention (Workshops)*. Springer, 2020, pp. 100–105.
- [34] T. Estienne, M. Lerousseau, M. Vakalopoulou, E. Alvarez Andres, E. Battistella, A. Carré, S. Chandra, S. Christodoulidis, M. Sahasrabudhe, R. Sun *et al.*, "Deep learning-based concurrent brain registration and tumor segmentation," *Frontiers in computational neuroscience*, vol. 14, p. 17, 2020.
- [35] T. Estienne, M. Vakalopoulou, E. Battistella, A. Carré, T. Henry, M. Lerousseau, C. Robert, N. Paragios, and E. Deutsch, "Deep learning based registration using spatial gradients and noisy segmentation labels," *Segmentation, Classification, and Registration of Multi-modality Medical Imaging Data*, vol. 12587, p. 87, 2020.
- [36] N. Gunnarsson, J. Sjölund, and T. B. Schön, "Learning a deformable registration pyramid," in *International Conference on Medical Image Computing and Computer-Assisted Intervention*. Springer, 2020, pp. 80–86.
- [37] D. Sun, X. Yang, M.-Y. Liu, and J. Kautz, "Pwc-net: Cnns for optical flow using pyramid, warping, and cost volume," in *Proceedings of the IEEE conference on computer vision and pattern recognition*, 2018, pp. 8934–8943.
- [38] T. C. Mok and A. C. Chung, "Large deformation diffeomorphic image registration with laplacian pyramid networks," in *International Conference on Medical Image Computing and Computer-Assisted Intervention*. Springer, 2020, pp. 211–221.
- [39] T. C. Mok and A. Chung, "Conditional deformable image registration with convolutional neural network," in *International Conference on Medical Image Computing and Computer-Assisted Intervention*. Springer, 2021, pp. 35–45.
- [40] V. Jaouen, P.-H. Conze, D. Guillaume, J. Bert, and D. Visvikis, "Regularized directional representations for medical image registration," 2021.
- [41] G. Lifshitz and D. Raviv, "Cost function unrolling in unsupervised optical flow," 2021.
- [42] S. Häger, S. Heldmann, A. Hering, S. Kuckertz, and A. Lange, "Variable fraunhofer mevis reglib comprehensively applied to learn2reg challenge," in *International Conference on Medical Image Computing and Computer-Assisted Intervention*. Springer, 2020, pp. 74–79.
- [43] M. Brudfors, Y. Balbastre, G. Flandin, P. Nachev, and J. Ashburner, "Flexible bayesian modelling for nonlinear image registration," in *International Conference on Medical Image Computing and Computer-Assisted Intervention*. Springer, 2020, pp. 253–263.
- [44] M. P. Heinrich, "Closing the gap between deep and conventional image registration using probabilistic dense displacement networks," in *International Conference on Medical Image Computing and Computer-Assisted Intervention*. Springer, 2019, pp. 50–58.
- [45] M. P. Heinrich and L. Hansen, "Highly accurate and memory efficient unsupervised learning-based discrete ct registration using 2.5 d displacement search," in *International Conference on Medical Image Computing and Computer-Assisted Intervention*. Springer, 2020, pp. 190–200.
- [46] W. Shao, Y. Pan, O. C. Durumeric, J. M. Reinhardt, J. E. Bayouth, M. Rusu, and G. E. Christensen, "Geodesic density regression for correcting 4dct pulmonary respiratory motion artifacts," *Medical Image Analysis*, p. 102140, 2021.
- [47] G. Balakrishnan, A. Zhao, M. R. Sabuncu, J. Guttag, and A. V. Dalca, "Voxelmorph: a learning framework for deformable medical image registration," *IEEE transactions on medical imaging*, 2019.
- [48] E. Gibson, F. Giganti, Y. Hu, E. Bonmati, S. Bandula, K. Gurusamy, B. Davidson, S. P. Pereira, M. J. Clarkson, and D. C. Barratt, "Automatic multi-organ segmentation on abdominal ct with dense v-networks," *IEEE transactions on medical imaging*, vol. 37, no. 8, pp. 1822–1834, 2018.
- [49] A. Hering, S. Häger, J. Moltz, N. Lessmann, S. Heldmann, and B. van Ginneken, "Cnn-based lung ct registration with multiple anatomical constraints," *Medical Image Analysis*, p. 102139, 2021.
- [50] M. Hoffmann, B. Billot, D. N. Greve, J. E. Iglesias, B. Fischl, and A. V. Dalca, "Synthmorph: learning contrast-invariant registration without acquired images," *IEEE Transactions on Medical Imaging*, 2021.
- [51] H. Siebert, L. Hansen, and M. P. Heinrich, "Evaluating design choices for deep learning registration networks," in *Bildverarbeitung für die Medizin 2021*. Springer, 2021, pp. 111–116.
- [52] M. P. Heinrich, M. Jenkinson, M. Bhushan, T. Matin, F. V. Gleeson, M. Brady, and J. A. Schnabel, "Mind: Modality independent neighbourhood descriptor for multi-modal deformable registration," *Medical image analysis*, vol. 16, no. 7, pp. 1423–1435, 2012.
- [53] E. Haber and J. Modersitzki, "Intensity gradient based registration and fusion of multi-modal images," in *International Conference on Medical Image Computing and Computer-Assisted Intervention*. Springer, 2006, pp. 726–733.
- [54] A. E. Kavur, N. S. Gezer, M. Barış, S. Aslan, P.-H. Conze, V. Groza, D. D. Pham, S. Chatterjee, P. Ernst, S. Özkan *et al.*, "Chaos challenge-combined (ct-mr) healthy abdominal organ segmentation," *Medical Image Analysis*, vol. 69, p. 101950, 2021.
- [55] J. Rühlhaak, T. Polzin, S. Heldmann, I. J. Simpson, H. Handels, J. Modersitzki, and M. P. Heinrich, "Estimation of large motion in lung ct by integrating regularized keypoint correspondences into dense deformable registration," *IEEE transactions on medical imaging*, vol. 36, no. 8, pp. 1746–1757, 2017.

A. Hering is with Fraunhofer MEVIS, Institute for Digital Medicine, 23562 Lübeck, Germany (email: alessa.hering@mevis.fraunhofer.de) and also with the Department of Radiology and Nuclear Medicine, Radboud University Medical Center, 6525 GA, Nijmegen, The Netherlands

L. Hansen, H. Siebert, C. Großbröhm, M.P. Heinrich are with the Institute of Medical Informatics, Universität zu Lübeck, 23562 Lübeck, Germany.

T. C. W. Mok and A. C. S. Chung are with the Department of Computer Science and Engineering, The Hong Kong University of Science and Technology, Hong Kong.

S. Häger, A. Lange, S. Kuckertz and S. Heldmann are with the Fraunhofer MEVIS, Institute for Digital Medicine, 23562 Lübeck, Germany

W. Shao and M. Rusu are with the Department of Radiology, Stanford University, Stanford CA 94305, USA.

S. Vesal and G. Sonn are with the Department of Urology, Stanford University, Stanford CA 94305, USA

T. Estienne is with the Université Paris-Saclay, CentraleSupélec, Mathématiques et Informatique pour la Complexité et les Systèmes, Inria Saclay, 91190, Gif-sur-Yvette, France and also with the Université Paris-

Saclay, Institut Gustave Roussy, Inserm, Radiothérapie Moléculaire et Innovation Thérapeutique, 94800, Villejuif, France.

M. Vakalopoulou is with the Université Paris-Saclay, CentraleSupélec, Mathématiques et Informatique pour la Complexité et les Systèmes, Inria Saclay, 91190, Gif-sur-Yvette, France.

L. Han is with the Department of Radiology and Nuclear Medicine, Radboud University Medical Center, 6525 GA, Nijmegen, The Netherlands.

Y. Huang is with the School of Automation, Nanjing University of Information Science and Technology, Nanjing 210044, China.

M.Brudfors is with the School of Biomedical Engineering and Imaging Sciences, King's College London, London, UK.

Y. Balbastre is with the Athinoula A. Martinos Center for Biomedical Imaging, Massachusetts General Hospital, USA and also with the Harvard Medical School, Boston, USA.

S. Joutard and M. Modat are with the King's College London, United Kingdom.

G. Lifshitz and D. Raviv are with the Tel Aviv University.

J. Lv and Q. Li are with the Britton Chance Center for Biomedical Photonics, Wuhan National Laboratory for Optoelectronics-Huazhong University of Science and Technology, Wuhan, Hubei 430074, China and also with the MoE Key Laboratory for Biomedical Photonics, Collaborative Innovation Center for Biomedical Engineering, School of Engineering Sciences, Huazhong University of Science and Technology, Wuhan, Hubei 430074, China.

V. Jaouen and D. Visvikis are with the UMR 1101 LaTIM, IMT Atlantique, Inserm, Brest, France.

C. Fourcade is with the Ecole Centrale de Nantes, LS2N, UMR CNRS 6004, Nantes, 44100, France and Keosys Medical Imaging, Saint Herblain, 44300, France.

M. Rubeaux is with the Keosys Medical Imaging, Saint Herblain, 44300, France.

W. Pan is with the Shenzhen International Graduate School, Tsinghua University, China.

Z. Xu is with the Department of Biomedical Engineering, The Chinese University of Hong Kong, Hong Kong, China.

B. Jian and F. De Benetti are with the Chair for Computer Aided Medical Procedures and Augmented Reality, Technische Universität München, Garching, Germany.

M. Wodzinski is with the AGH University of Science and Technology, Department of Measurement and Electronics, Krakow, Poland and also with the University of Applied Sciences Western Switzerland (HES-SO Valais), Information Systems Institute, Sierre, Switzerland.

N. Gunnarsson and Jens Sjölund are with the Department of Information Technology, Uppsala University, Uppsala, Sweden and also with Elekta Instrument AB, Stockholm, Sweden.

H. Qiu and Z. Li are with the Department of Computing at Imperial College London.

A. Hoopes is with the Athinoula A. Martinos Center for Biomedical Imaging, Massachusetts General Hospital, USA.

I. Reinertsen is with the Dept. Health Research, SINTEF Digital, Trondheim, Norway.

Y. Xiao is with the Western University, London, Canada.

B.Landman and Y. Huo are with the Department of Electrical and Computer Engineering, Vanderbilt University.

N Lessmann and K. Murphey and B van Gincken are with the Department of Radiology and Nuclear Medicine, Radboud University Medical Center, 6525 GA, Nijmegen, The Netherlands.

A. V. Dalca is with the Computer Science and Artificial Intelligence Lab, MIT, USA, the Martinos Center for Biomedical Imaging, Massachusetts General Hospital, USA and also with the Harvard Medical School, Boston, USA.